Supplemental information for Tuning of Spin Reorientation and Spin Switching in Sm-doped $NdFeO_3$

Sk Samim Ahammad*
Department of Physics, Indian Institute of Science, Bangalore, India

C.M.N. Kumar
Institute of Nuclear Physics, Polish Academy of Sciences, Krakow, Poland

Michał Rams
Jagiellonian University, Kraków, Poland

Suja Elizabeth
Department of Physics, Indian Institute of Science, Bangalore, India

February 7, 2026

*Email: sksamima@iisc.ac.in

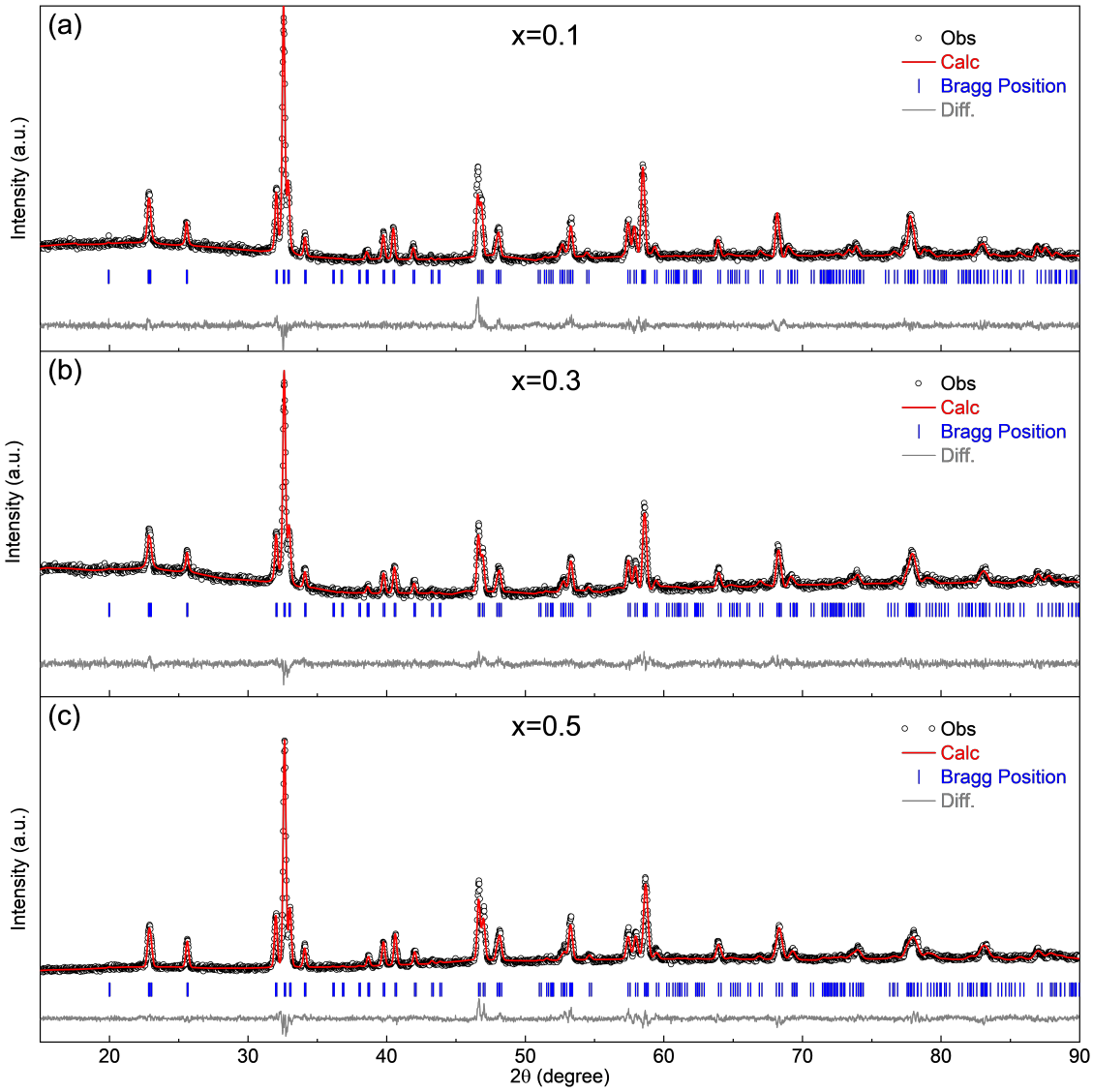

Figure S1: Rietveld refinement results of PXRD patterns of $Nd_{1-x}Sm_xFeO_3$ ($x = 0.1, 0.3, 0.5$) samples.

Table S1: Structural parameters, selected atomic coordinates, Fe–O bond distances, O–Fe–O bond angles, Rietveld refinement reliability factors, and Goldschmidt tolerance factor t for $Nd_{1-x}Sm_xFeO_3$ compositions.

Composition (x)	0.1	0.3	0.5
Lattice parameters			
a (Å)	5.4426(2)	5.4313(3)	5.4226(2)
b (Å)	5.5852(2)	5.5865(3)	5.5906(2)
c (Å)	7.7531(3)	7.7402(4)	7.7307(3)
V (Å^3)	235.68(2)	234.85(2)	234.36(2)
Atomic coordinates (fractional)			
Nd/Sm x	0.9862(7)	0.9874(8)	0.9853(7)
Nd/Sm y	0.0489(3)	0.0507(3)	0.0524(3)
O(1) x	0.097(3)	0.098(4)	0.089(3)
O(1) y	0.478(3)	0.479(4)	0.476(3)
O(2) x	0.715(3)	0.717(4)	0.722(4)
O(2) y	0.291(3)	0.303(3)	0.289(3)
O(2) z	0.033(2)	0.040(3)	0.041(2)
Fe–O bond distances (Å)			
Fe–O1	2.013(6)	2.010(6)	1.997(4)
Fe–O2 (short)	1.96(2)	1.92(2)	1.94(2)
Fe–O3 (long)	2.02(19)	2.09(2)	2.04(2)
O–Fe–O bond angles (deg)			
O1–Fe–O2	92.6(1)	91.3(14)	89.4(12)
O1–Fe–O2	85.5(2)	86.9(11)	87.4(10)
O1–Fe–O2	87.4(12)	88.7(12)	90.6(10)
O1–Fe–O2	94.5(13)	93.1(13)	92.6(11)
O2–Fe–O2	90.2(13)	90.6(13)	89.9(13)
O2–Fe–O2	89.8(15)	89.4(13)	90.1(15)
Rietveld refinement reliability factors			
χ^2	1.67	1.26	1.91
R_{wp}	17.2	18.3	15.8
R_{exp}	13.3	16.3	11.4
Goldschmidt tolerance factor			
t	0.9222	0.9201	0.9180

Notes: The crystal structure was refined in the orthorhombic *Pbnm* setting (No. 62). The Wyckoff positions are as follows: A-site (Nd/Sm) at 4c $(x, y, 1/4)$, Fe at 4b $(0, 0.5, 0)$, O(1) at 4c $(x, y, 1/4)$, and O(2) at 8d (x, y, z).

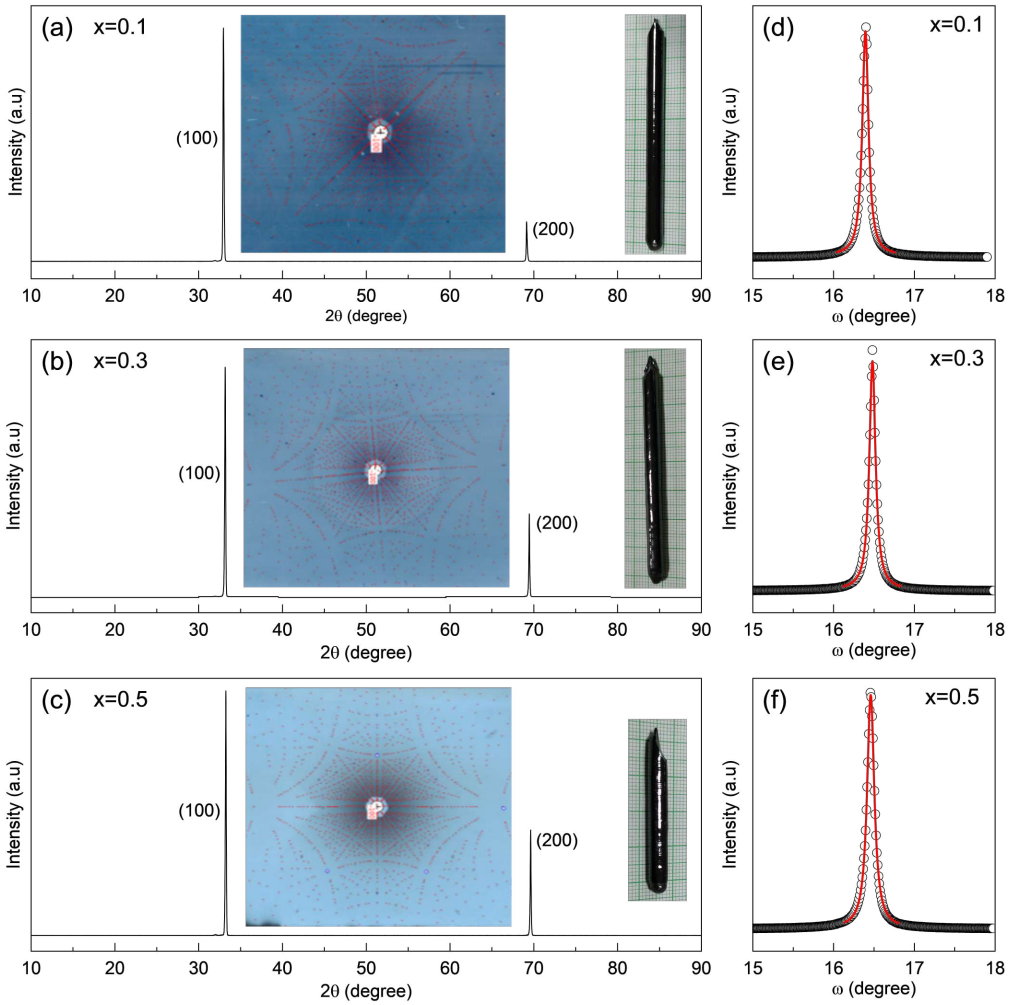

Figure S2: (a–c) XRD of the oriented crystals of ($Nd_{1-x}Sm_xFeO_3$) cut into discs with the crystallographic ($h00$) plane perpendicular. Insets show Laue images of the ($h00$) plane and photographs of the grown crystals. (d–f) Rocking curve of (100) plane; black circles are experimental data and red curves are pseudo-Voigt fits.

Table S2: FWHM of rocking curves shown in figure S2(d-f).

Composition x	0.1	0.3	0.5
FWHM	0.092(4)	0.092(1)	0.104(2)

Supplementary note 1: Explanation of different magnetization protocols.

ZFC (Zero-Field Cooled): The sample is cooled from a high temperature to the lowest measurement temperature (2 K for $x = 0.5$) without applying any magnetic field. At 2 K, a magnetic field is applied, and the magnetization data are recorded during subsequent heating under that applied field.

FCC (Field-Cooled Cooling): The sample is cooled from a high temperature down to 2 K under an applied magnetic field, and the magnetization data are recorded during the cooling process.

FCW (Field-Cooled Warming): After cooling the sample from a high temperature to 2 K under an applied magnetic field, the sample is heated with the same field, and the magnetization data are recorded as a function of temperature.

NFC (Negative Field Cooled): The sample is cooled from a high temperature to 2 K under a negative magnetic field. At 2 K, the field is switched to a positive value, and the magnetization data are collected during the subsequent heating process.

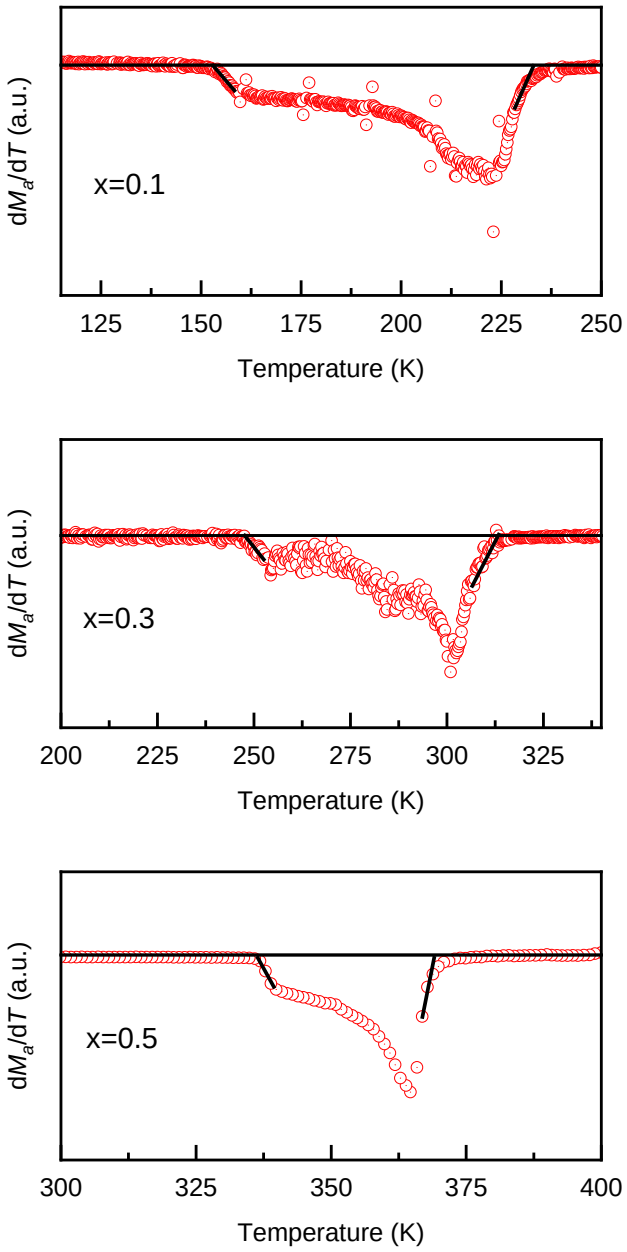

Figure S3: Temperature derivative of the magnetization along the a-axis under field-cooled cooling (FCC) conditions for $Nd_{1-x}Sm_xFeO_3$.

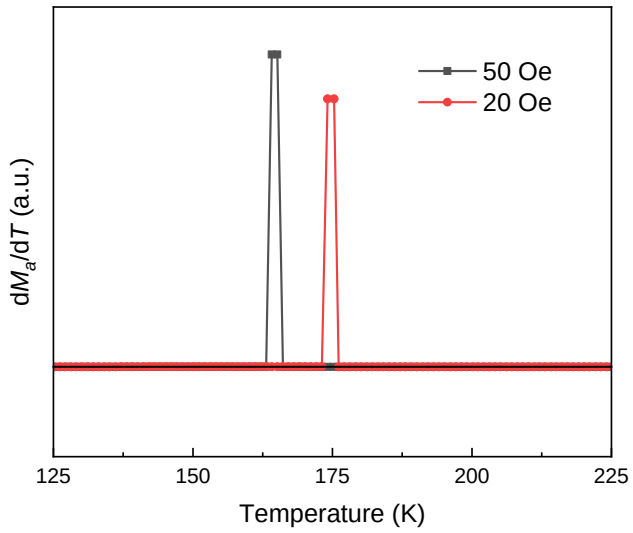

Figure S4: Temperature derivative of the magnetization along the a-axis under zero-field-cooled (ZFC) conditions.

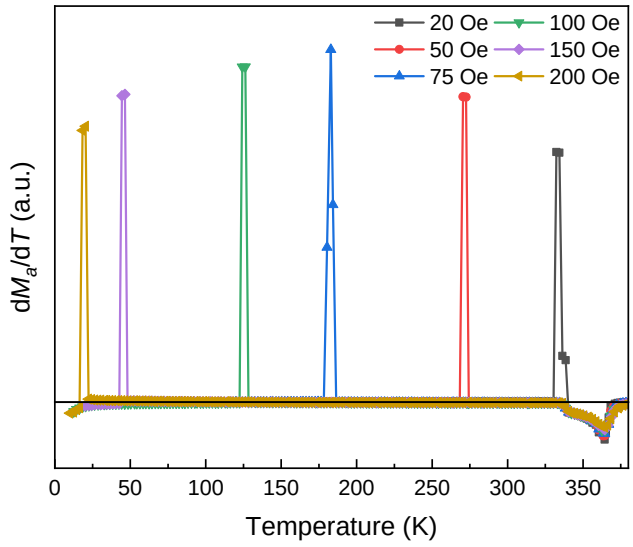

Figure S5: Temperature derivative of the magnetization along the a-axis under negative-field-cooled (NFC) conditions.

Table S3: T_{SR} extracted from the extrapolation of the dM_a/dT curve measured with the FCC protocol.

Composition	T_{SR1} (K)	T_{SR2} (K)
0.1	233.2	152.9
0.3	313.3	247.6
0.5	369.2	336.3

Table S4: T_{ZFC} extracted from the peak position of the dM_a/dT curve measured with the ZFC protocol.

Applied Field (Oe)	Temperature (K)
20	174.7
50	164.6

Table S5: T_{ZFC} extracted from the peak position of the dM_a/dT curve measured with the NFC protocol.

Applied Field (Oe)	Temperature (K)
20	333.3
50	271.5
75	182.9
100	125.3
150	45.4
200	19.4

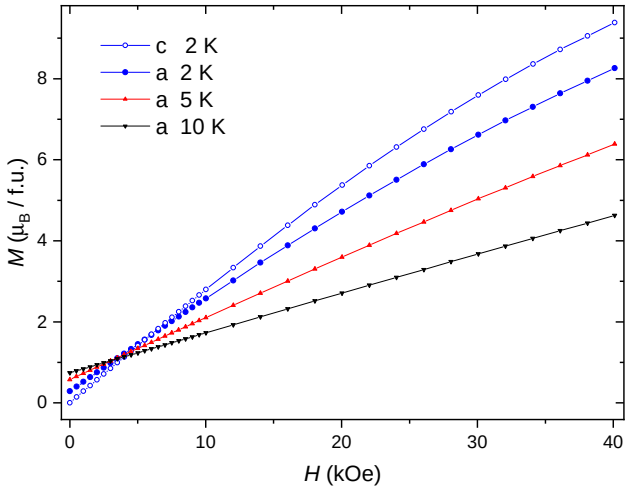

Figure S6: Magnetization of $Nd_{0.5}Sm_{0.5}FeO_3$ at low temperatures. The field where M is temperature independent gives the molecular field of Fe moments at the rare-earth site (see main text).

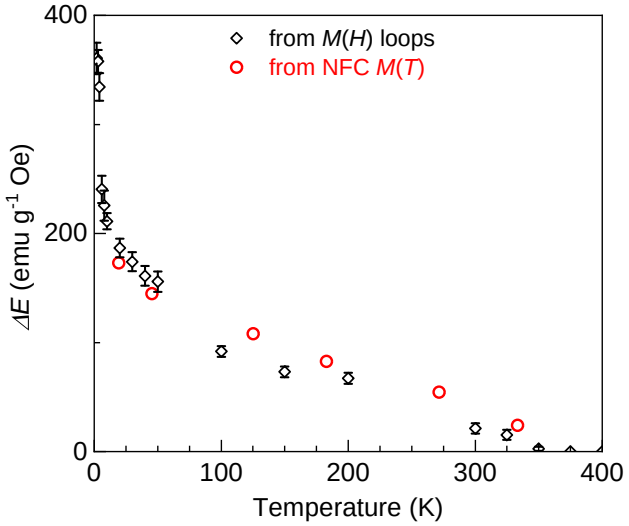

Figure S7: Temperature dependence of the switching energy barrier in $Nd_{0.5}Sm_{0.5}FeO_3$. This was calculated as $\Delta E = H\Delta M/2$, at the switching of magnetization of the hysteresis loop, and at the switching of magnetization during warming the sample at different fields following NFC (data in Figures 4 and 6).

Supplementary note 2: Magnetization conservation across the spin-switching transition

To verify the classification of the observed transition as type-I spin switching, the magnetization values immediately before and after the switching event were evaluated for both zero-field-cooled (ZFC) and negative-field-cooled (NFC) measurement protocols.

Tables S6 and S7 summarize the magnetization measured just below and just above the spin-switching temperature T_{SSW}, together with the corresponding change ΔM. In all cases, the absolute value of the magnetization remains nearly conserved across the switching transition, with only a reversal of its sign.

This behavior is a defining characteristic of type-I spin switching, arising from the abrupt reconfiguration of two antiparallel magnetic sublattices when the Zeeman energy overcomes the anisotropy energy barrier.

Table S6: ΔM in the ZFC protocol.

Applied field (Oe)	Magnetic moment before switching ($\mathrm{emu\,g^{-1}}$)	Magnetic moment after switching ($\mathrm{emu\,g^{-1}}$)	ΔM ($\mathrm{emu\,g^{-1}}$)
20	−1.031	1.028	2.059
50	−1.038	1.041	2.079

Table S7: ΔM in the NFC protocol.

Applied field (Oe)	Magnetic moment before switching ($\mathrm{emu\,g^{-1}}$)	Magnetic moment after switching ($\mathrm{emu\,g^{-1}}$)	ΔM ($\mathrm{emu\,g^{-1}}$)
20	−0.905	0.875	1.78
50	−0.956	0.949	1.905
75	−1.002	0.998	2.00
100	−1.003	1.003	2.06
150	−0.916	0.928	1.844
200	−0.822	0.856	1.678

Supplementary Note 3: Benchmarking of T_{SSW} tunability

Table S8 summarizes representative reports of spin-switching tunability in rare-earth orthoferrites. Because the experimental protocols vary across studies (e.g., ZFC, FCC, FCW, and protocol variants involving field changes during cooling), the quantity $\Delta T_{SSW}/\Delta H$ should be regarded as an effective tuning metric extracted from the reported field/protocol variation rather than a universal material constant.

For the present work, ΔT_{SSW} is defined as the difference between the switching temperatures obtained under the ZFC and NFC protocols at the same warming field (H_{warm} = 20 Oe), i.e. $\Delta T_{SSW} \approx 158$ K. ΔH corresponds to the magnitude of the negative cooling field used to imprint the bias ($|H_{cool}| = 20$ Oe), yielding $\Delta T_{SSW}/\Delta H \approx 7.9\ \mathrm{K\,Oe^{-1}}$.

Table S8: Condensed comparison of spin-switching tunability reported for representative orthoferrites. ΔT_{SSW} and ΔH are extracted from the protocol/field variation described in each reference.

Material (Ref.)	ΔH (Oe)	ΔT_{SSW} (K)	$\Delta T_{SSW}/\Delta H$ ($\mathrm{K\,Oe^{-1}}$)	Brief protocol note
$Nd_{0.5}Sm_{0.5}FeO_3$ (this work)	20	158	7.9	ZFC vs NFC at $H_{warm} = 20$ Oe
$DyFeO_3$ (1)	200	100	0.5	Switching enabled by applying −200 Oe at 300 K prior to cooling
$SmFeO_3$ (2)	50	77.5	1.55	ZFC: 356 K (250 Oe) to 278.5 K (300 Oe)
$ErFeO_3$ (3)	20000	25	0.00125	FCW at 50 Oe; ±10 kOe applied at 85 K
$NdFeO_3$ (4)	400	20	0.05	ZFC: ∼20 K shift from 100 to 500 Oe

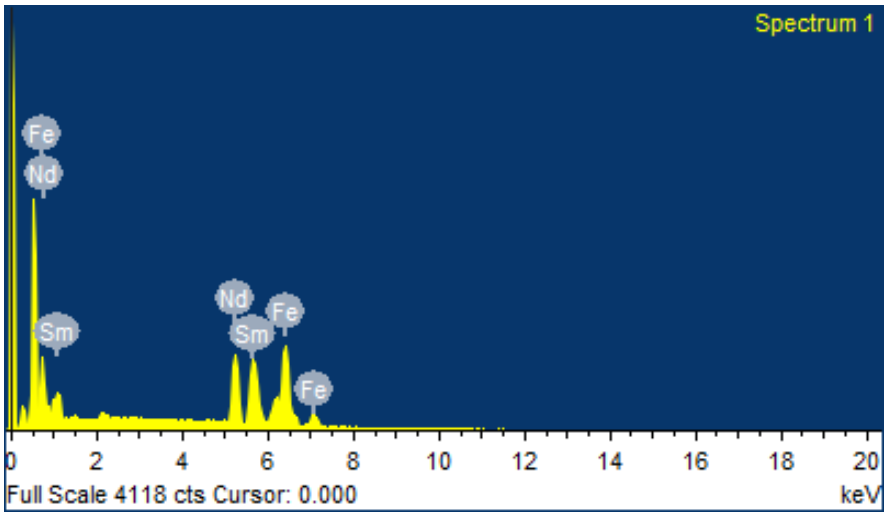

Figure S8: EDS spectrum of $Nd_{0.5}Sm_{0.5}FeO_3$

References

[1] S. Cao, L. Chen, W. Zhao, K. Xu, G. Wang, Y. Yang, B. Kang, H. Zhao, P. Chen, A. Stroppa, *et al.*, "Tuning the weak ferromagnetic states in dysprosium orthoferrite," *Scientific Reports*, vol. 6, p. 37529, 2016.

[2] S. Cao, H. Zhao, B. Kang, J. Zhang, and W. Ren, "Temperature-induced spin switching in $SmFeO_3$ single crystal," *Scientific Reports*, vol. 4, p. 5960, 2014.

[3] I. Fita, R. Puzniak, E. Zubov, P. Iwanowski, and A. Wiśniewski, "Temperature-driven spin switching and exchange bias in the $ErFeO_3$ ferrimagnet," *Physical Review B*, vol. 105, p. 094424, 2022.

[4] S. Yuan, W. Ren, F. Hong, Y. Wang, J. Zhang, L. Bellaiche, S. Cao, and G. Cao, "Spin switching and magnetization reversal in single-crystal $NdFeO_3$," *Physical Review B*, vol. 87, p. 184405, 2013.